

Recent simulations of Toroidal Alfvén Eigenmodes on JET with the Gyrokinetic Toroidal Code

V. Aslanyan¹, M. Porkolab¹, N. Fil¹, S. Taimourzadeh², L. Shi², Z. Lin², G. Dong³,
 P. Puglia⁴, S. E. Sharapov⁵, J. Mailloux⁵, M. Tsalas⁵, M. Maslov⁵, A. Whitehead⁵,
 R. Scannell⁵, S. Gerasimov⁵, S. Dorling⁵, S. Dowson⁵, H. K. Sheikh⁵, T. Blackman⁵,
 G. Jones⁵, A. Goodyear⁵, K. K. Kirov⁵, R. Dumont⁶, P. Blanchard⁴,
 A. Fasoli⁴, D. Testa⁴, and JET Contributors*

EUROfusion Consortium, JET, Culham Science Centre, Abingdon, OX14 3DB, UK

¹*MIT PSFC, 175 Albany Street, Cambridge, MA 02139, US*

²*Department of Physics and Astronomy, UCI, CA 92697, US*

³*PPPL, Princeton University, Princeton, NJ 08543, US*

⁴*Swiss Plasma Center (SPC), CH-1015 Lausanne, Switzerland*

⁵*CCFE, Culham Science Centre, Abingdon, OX14 3DB, UK*

⁶*CEA, IRFM, F-13108 Saint-Paul-lez-Durance, France*

The impact of energetic particles on the stability of Toroidal Alfvén Eigenmodes (TAEs) in fusion grade plasmas is not well understood and demands further experimental and theoretical study. Efforts have recently been undertaken on JET to develop a scenario to observe TAEs in a DT plasma on JET[1], with particular emphasis on unstable TAEs which can be unambiguously attributed to fusion α s. The Gyrokinetic Toroidal Code (GTC)[2] self-consistently treats bulk ions, energetic ions, electrons and fields in tokamaks, making it well suited to support these experimental efforts on JET. We present recent efforts to simulate unstable TAEs observed passively and stable TAEs excited resonantly by the recently upgraded Alfvén Eigenmode Active Diagnostic (AEAD)[3].

GTC uses a δf particle-in-cell approach to treat bulk and “fast” ions gyrokinetically, or using a reduced MHD-like model. Electrons are treated either with an adiabatic or hybrid-kinetic approach, as specified. These three particle species are assumed to have independent, spatially-dependent Maxwellian distributions. The ALCON[4] code is used to compute the Alfvén Continuum and in particular identify the TAE gap. A synthetic antenna is also available to resonantly excite modes, analogously to external excitors, such as the AEAD. In GTC, the synthetic antenna imposes an electrostatic perturbation inside the bulk plasma consisting of a number of toroidal and poloidal spatial components and oscillating sinusoidally in time.

We have chosen to analyze an unstable TAE, at 5.2 s in JPN #92416 conducted in late 2016

*See the author list of X. Litaudon et al., Nucl. Fusion **57**, 102001 (2017).

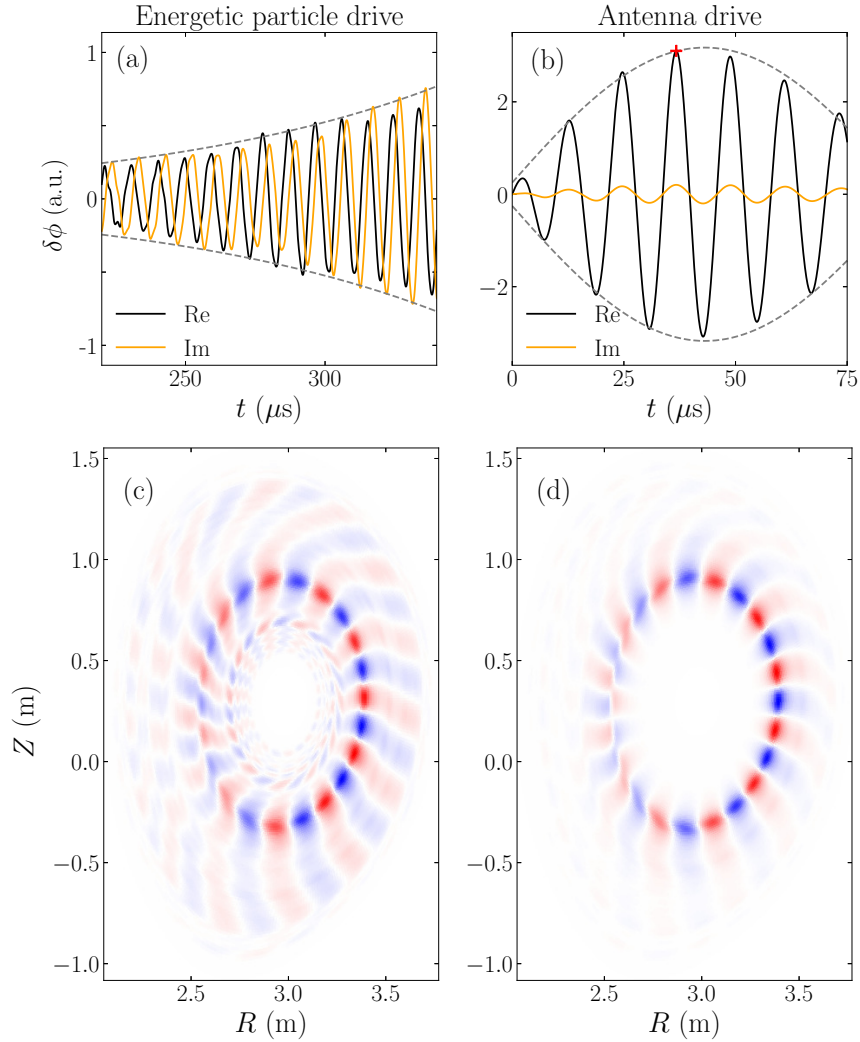


Figure 1: Real and imaginary components of the electrostatic potential perturbation of (a) energetic particle driven and (b) synthetic antenna driven TAE with $n = 5$. The red cross in (b) indicates the time when the peak amplitude is taken for the purposes of damping rate calculation (see below). The corresponding spatial mode structures are given by (c) and (d) respectively.

with plasma composed of deuterium. Energetic ions accelerated by Ion Cyclotron Resonance Heating (ICRH) are responsible for destabilizing the modes. The chosen TAE has toroidal mode number $n = 5$ and observed (lab frame) frequency $f_{\text{LAB}} = 154$ kHz. We deduce the plasma rotation frequency to be ~ 8 kHz from observations of other concurrent unstable TAEs by assuming that neighbouring harmonics have approximately equal frequencies in the plasma frame.

For the simulation parameters, the electron density n_e and temperature T_e are taken from the High Resolution Thomson Scattering diagnostic. The density of “fast” ions is taken from an ICRH absorption code, and an effective temperature (thereby approximating their velocity

distribution as Maxwellian) is deduced from their energy content. At the flux surface where the TAE peaks, these quantities are $n_{fi}/n_e = 4.9 \times 10^{-3}$ and $T_{fi} = 550$ keV respectively. The remaining bulk ion density is taken from quasineutrality and we assume $T_i \simeq T_e$, based on spectroscopic measurements. GTC simulations with these parameters and hybrid-kinetic electrons are shown in Fig. 1a exhibit an exponentially growing TAE, with a ballooning spatial structure given in Fig. 1c. Analysis of the oscillations gives a plasma frame frequency of 110 kHz, consistent with passive observations, and a net growth rate $\gamma/\omega = +1.38\%$.

The rate of electron Landau damping was deduced by repeating this simulation with the adiabatic electron model; the increase in growth rate is attributable to a lack of damping by electrons. To quantify the effect of radiative and ion Landau damping, we repeat this simulation without a population of energetic ions (but still with quasineutrality), using a synthetic antenna with a spatial structure shown in Fig. 1d; note how the structure is chosen to closely resemble the unstable TAE. The amplitude of such driven oscillations peaks in time, as shown in Fig. 1b. The spectral distribution of such peaks is given in Fig. 2, with an appropriate fit function allowing the damping rate to be deduced. The simulation is performed twice, with the reduced MHD-like and full gyrokinetic models for the ions; differences in the damping rate are directly attributable to ion Landau damping being present in the latter case only. Results for the damping rate analysis are summarized in Table 1.

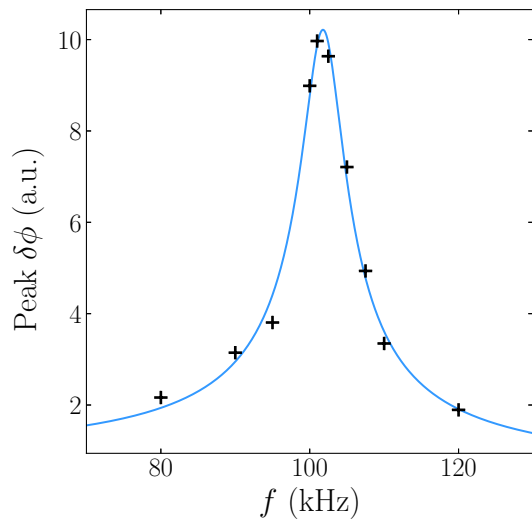


Figure 2: *Spectral response to synthetic antenna excitation in GTC for a TAE with $n = 5$. Peak amplitudes as a function of frequency are given by crosses, the fit function with $f = 101$ kHz and $\gamma/\omega = -2.82\%$ by the solid line.*

Mechanism	Drive/Damping γ/ω	
	Total	Net
Continuum	$\sim 0\%$	$\sim 0\%$
Radiative	-1.18%	-1.18%
Ion Landau	-2.82%	-1.64%
Energetic particle	$+1.47\%$	$+4.29\%$
Electron Landau	$+1.38\%$	-0.09%

Table 1: *Drive and damping mechanisms and corresponding total drive or damping rate, obtained directly from the corresponding simulation, used to deduce the net rate for each mechanism.*

We repeat this process for a TAE detected through resonant excitation by AEAD antennas in the same JET pulse. The toroidal mode number could not be accurately measured due to a lack of functioning pick-up coils at the end of the JET campaign, so we simulate four candidate modes with $n = 5$ and $n = 6$. The frequencies and damping rates of these modes are shown relative to the measured values and the Alfvén Continuum in Fig. 3. Note that the plasma rotation was negligible at this time. The frequency and damping rate of the $n = 5, m = 5, 6$ mode closely match the antenna measurements.

Acknowledgements This work has been part-funded by the RCUK Energy Programme [grant number EP/P012450/1]. Support for the MIT group was provided by the US DOE under Grant Number DE-FG02-99ER54563, and by SciDAC ISEP Center. This work used resources of the Oak Ridge Leadership Computing Facility at the Oak Ridge National Laboratory (DOE Contract No. DE-AC05-00OR22725) and the National Energy Research Scientific Computing Center (DOE Contract No. DE-AC02-05CH11231). This work has been carried out within the framework of the EUROfusion Consortium and has received funding from the Euratom research and training programme 2014-2018 under grant agreement No 633053. The views and opinions expressed herein do not necessarily reflect those of the European Commission.

References

- [1] R. Dumont, J. Mailloux, V. Aslanyan, *et al.*, Nucl. Fusion (in press) (2018).
- [2] Z. Wang, Z. Lin, I. Holod, W. W. Heidbrink, *et al.*, Phys. Rev. Lett. **111**, 145003 (2013).
- [3] P. Puglia, W. Pires de Sa, P. Blanchard, *et al.*, Nucl. Fusion **56**, 112020 (2016).
- [4] W. Deng, Z. Lin, I. Holod, Z. Wang, Y. Xiao, and H. Zhang, Nucl. Fusion **52**, 043006 (2012).

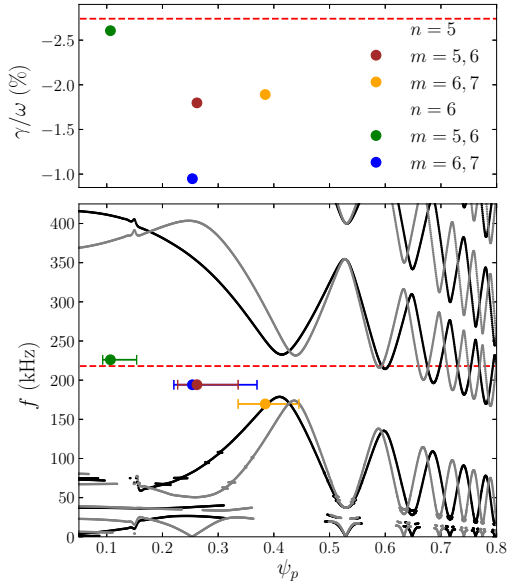


Figure 3: (Lower panel) Branches of the Alfvén continuum for $n = 5$ (black) and $n = 6$ (grey) showing the TAE gap. The frequencies and spatial widths of modes probed by a synthetic antenna, with n and pairs of m as indicated, are shown relative to the continuum. (Upper panel) The corresponding damping rates. The red lines correspond to the frequency and damping rate in the respective panels.